Progress In Electromagnetics Research, PIER 97, 75–93, 2009

ON QUANTITATIVE MICROWAVE TOMOGRAPHY OF FEMALE BREAST

I. Catapano, L. Di Donato, L. Crocco, and O. M. Bucci †

Consiglio Nazionale delle Ricerche
Istituto per il Rilevamento Elettromagnetico dell'Ambiente (IREA)
Via Diocleziano 328, Napoli 80124, Italy

A. F. Morabito and T. Isernia

Dipartimento di Informatica, Matematica, Elettronica e Trasporti (DIMET)
Università Mediterranea di Reggio Calabria
Via Graziella, Loc. Feo di Vito, Reggio Calabria 89100, Italy

R. Massa

Dipartimento di Scienze Fisiche
Università degli Studi di Napol Federico II
Via Cintia, Napoli 80126, Italy

Abstract—Microwave tomography deserves attention in biomedical imaging, owing to its potential capability of providing a morphological and functional assessment of the inspected tissues. However, such a goal requires the not trivial task of solving a non linear inverse scattering problem. In this paper, the factors affecting the complexity of the inverse problem are exploited to trace guidelines aimed at setting the matching fluid, the frequency range and the number of probes in such a way that the dielectric parameters of female breast tissues can be reliably retrieved. Examples, concerning 2D realistic numerical phantoms obtained by NMR images, are given to asses a posteriori the effectiveness of the proposed guidelines.

Corresponding author: L. Crocco (crocco.l@irea.cnr.it).
† Also with DIBET — Università degli Studi di Napol Federico II Via Claudio 21, Napoli 80125, Italy.

1. INTRODUCTION

In the recent years, there has been a growing interest in exploiting microwave imaging techniques for breast cancer screening [1–4]. As a matter of fact, these latter would provide a non-invasive diagnostics tool having the potential capability of achieving a functional assessment, from which infer not only the morphology but also the dielectric features of the detected anomalies. In such a framework, this capability would allow to overcome the intrinsic limitations in terms of false positives/negatives discrimination of X-ray mammography, the standard technology used in most screening prevention programs [5, 6]. Accordingly, several strategies, mainly assuming a simplified model of the breast or *a priori* information on its structure, have been proposed for cancer detection [7–9] and its morphological and functional characterization [10–14].

On the other hand, some recent experimental studies have pointed out that, in the microwave frequency range, while there is a remarkable difference amongst the dielectric features of normal fatty breast tissues and those of tumors [15–17], while the properties of these latter are close to those of mammary ducts [16, 17]. As a consequence, it may be very hard to discriminate normal and cancerous tissues, for this last case. To overcome this drawback, some authors have proposed the adoption of contrast agents, such as carbon nanotubes, to restore a significant variation amongst the dielectric properties of different tissues [18], while other authors have considered hybrid imaging modalities combining microwaves and acoustic excitations [19, 20].

The above described framework shows clearly that the problem of reconstructing the dielectric parameters of breast tissues is a necessary preliminary step to tackle. As a matter of fact, it provides useful *a priori* information, which allow to enhance the cancer imaging capabilities of microwave screening tools and may also positively act on the performances of strategies exploiting contrast agents or hybrid excitations. However, achieving a functional characterization of breast tissues is an ambitious aim requiring to face a non-linear and ill-posed problem that, as well known, is affected by instabilities and occurrence of "false solutions" [21].

Typically, non-linear inverse problems are cast as the minimization (or the maximization) of a proper cost functional, so that the practical task to pursue is the achievement of the *global* optimum of such a functional [22, 23]. Unfortunately, owing to the large number of unknown parameters to be determined, global optimization procedures may be unfeasible and local algorithms are adopted. As a consequence, the minimization process is strongly dependent on the starting guess

and may lead to a *local* minimum, corresponding to a reconstruction different from the actual scenario. This difficulty, which is of course detrimental for any inverse scattering problem, is crucial in the framework of medical imaging, as it ultimately influences the reliability of the diagnosis.

In this respect, it is worth remarking that, unlike what happens in other cases (such as for instance subsurface imaging), the experimental scenario for breast imaging is, to some extent, a *degree of freedom*. Hence, a proper design of the screening tool can (in principle) improve the capabilities of microwave imaging diagnosis.

According to this observation, by reasoning on the factors affecting the complexity of the inverse problem at hand, we will give some guidelines for a suitable choice of the matching fluid as well as of the working frequency band. In addition, since one is interested in having an experimental system as simple as possible, these two information will allow us to determine a minimal number of antennas. Due to the complexity of the screening tool and the high variability of the involved materials, the definition of an exact and general model of the scattering scenario is a difficult task. Therefore, the proposed analysis exploits a simplified model whose validity is checked a posteriori through the numerical examples. In particular, the effectiveness of the proposed guidelines is shown in the canonical 2D case, with respect to nuclear magnetic resonance (NMR) images based anthropomorphic numerical phantoms [24].

The inverse scattering problem is faced without requiring any *a priori* information on the breast structure and the adopted imaging procedure is based on a modified gradient inversion scheme in which ill-conditioning is defeated by means of a suitable initialization of the iterative process. To this end, the linear sampling method (LSM) [25] is adopted to obtain a preliminary morphologic characterization of the breast. In addition, a regularization by projection strategy, in which the unknown contrast function is represented by means of Fourier harmonics basis functions [26], is exploited.

The paper is organized as follow. Section 2 states the problem at hand, while the inversion strategy is summarized in Section 3. The parameters affecting the breast microwave imaging are discussed in Section 4, where some guidelines to properly set them are also traced. Numerical examples corroborating the achievable reconstruction capabilities are given in Section 5. Conclusions follow.

2. STATEMENT OF THE PROBLEM

The measurement system usually proposed for microwave breast cancer screening requires that the patient lies in a prone position with the breast immersed in a beaker filled with a matching fluid. Multiview, multistatic and multifrequency data are collected by means of a circular array of probes immersed inside the fluid and located all around the breast [7–14]. A sketch of this kind of measurement configuration is given in Fig. 1, where Ω is the investigated domain, Σ the measurement curve and ϵ_f and σ_f the relative permittivity and conductivity of the fluid, respectively.

As the paper aims at assessing how a proper design of the microwave screening tool makes it possible accurate reconstructions of the dielectric features of breast tissues, the canonical two dimensional scalar case is considered.

By assuming that the incident field is polarized along the invariance axis, that is the z-axis, for each position of the primary source at a given frequency, the scattering problem is cast by means of the following source type integral equations:

$$J(\mathbf{r}) - \chi(\mathbf{r}) E_{inc}(\mathbf{r}) = k_b^2 \chi(\mathbf{r}) \int_\Omega G\big(\mathbf{r}-\mathbf{r}'\big) J\left(\mathbf{r}'\right) dr' = \chi \mathbf{A}_i[J],\ \mathbf{r} \in \Omega \quad (1)$$

$$E_s(\mathbf{r}) = k_b^2 \int_\Omega G\left(\mathbf{r}-\mathbf{r}'\right) J\left(\mathbf{r}'\right) dr' = \mathbf{A}_e[J],\ \mathbf{r} \in \Sigma, \quad (2)$$

where J is the induced current into Ω, k_b is the background wave number at the working frequency, G is the scalar Green's function for

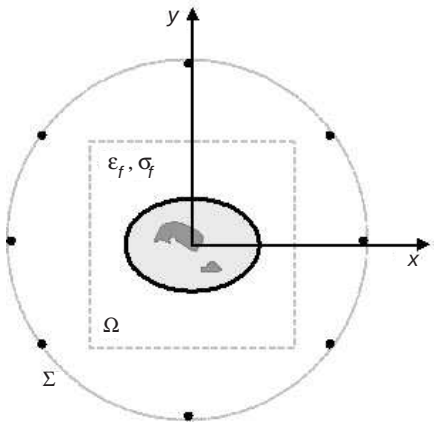

Figure 1. Sketch of the reference scenario.

homogeneous media, whose electromagnetic features are those of the matching fluid [27]. E_{inc} is the incident field in Ω and E_s the scattered field on Σ, i.e., the measured data in each scattering experiment. $\mathbf{A}_i : L^2(\Omega) \rightarrow L^2(\Omega)$ and $\mathbf{A}_e : L^2(\Omega) \rightarrow L^2(\Sigma)$ are the internal and external radiation operators relating the contrast source to the scattered field in Ω and on Σ, respectively. The contrast χ relates the complex permittivity of the breast to that of the matching fluid.

To reconstruct the morphology and dielectric features of breast tissues one has to solve the system of coupled integral Equations (1) and (2) in terms of the unknown χ, that is a non linear and ill-posed problem [21].

3. INVERSION STRATEGY

The imaging problem is tackled by adopting a two-step inversion strategy. In particular, the linear sampling method (LSM) [25] is initially exploited to achieve a morphological characterization of the breast, that is used to define the starting guess of the iterative inversion procedure. By addressing the reader to [25, 28, 29] for an accurate description of the LSM and its utility in the framework of quantitative imaging problems, we only remind that LSM is a general and computationally effective approach to reconstruct the targets morphology through the regularized solution of a linear inverse problem. Since this method is not able to provide any information on the dielectric parameters of the objects, we assign to the reconstructed breast' shape an arbitrary constant value of permittivity and conductivity to provide the starting guess for the contrast χ.

The second step of the inversion strategy aims at retrieving the dielectric features of the breast tissues and it is based on the contrast source inversion (CSI) method [30]. In particular, the conjugate gradient fast Fourier transform (CG-FFT) technique is used to minimize, at a fixed frequency, the cost functional:

$$\Phi(\chi, J^\nu) = \sum_{\nu=1}^{N_v} \frac{\|J^\nu - \chi E^v_{inc} - \chi \mathbf{A}_i[J^\nu]\|^2}{\|E^v_{inc}\|^2} + \sum_{\nu=1}^{V} \frac{\|E^\nu_s - \mathbf{A}_e[J^\nu]\|^2}{\|E^\nu_s\|^2}, \quad (3)$$

where $v = 1, \ldots, N_v$ denotes the v-th scattering experiment in a multiview set-up. The first term of the cost functional represents the misfit in the object Equation (1), while the second one the misfit in the data Equation (2). According to the minimization scheme in [26], the gradient update is simultaneously performed for both the unknown contrast χ and the contrast sources $J^1, \ldots, J^{N_v}$. Note this is different from the usual CSI minimization, where alternate updates are considered [30].

The dispersive behavior of tissues and matching fluid is described through a maxwellian model, i.e., it is taken into account by means of the complex equivalent permittivity $\epsilon_{eq} = \epsilon_0(\epsilon - j\sigma/(\omega\epsilon_0))$. Moreover, the minimization is carried out by taking into account that relative permittivities less than 1 and negative conductivities are not physically possible. In addition, a *regularization by projection* strategy is applied, so that the unknown contrast is represented by means of the spatial Fourier harmonics, instead of the commonly used pulse basis functions [30]. This is a crucial aspect in the framework of non-linear inverse problems, where the occurrence of local minima in the iterative process can be reduced, or even avoided, if the ratio between the number of unknowns and the amount of independent data is sufficiently large [31]. In this respect, we look for the unknown contrast belonging to a finite dimensional space, whose dimension is compatible with the dimension of the independent data. Since the amount of independent information increases with the frequency [32–34], the number of Fourier harmonics is progressively enlarged while the inversion procedure evolves.

Finally, in order to take advantage of frequency diversity while not increasing the overall computational complexity, the *frequency hopping* procedure is adopted [35], in which the inversion algorithm is first performed at low frequency and the result is used as initial guess at higher frequencies. At the lowest processed frequency, the initial guess is obtained, as stated before, from the LSM.

4. PARAMETERS AFFECTING THE EFFICACY OF FEMALE BREAST IMAGING TECHNIQUES

This section aims at providing some guidelines to set the working frequency range, the matching fluid and the number of transmitting and receiving probes. As a matter of fact, provided practical realization constraints are taken into account, these parameters are degrees of freedom for the screening tool and can contribute significantly in reducing/increasing the complexity of the inverse scattering problem at hand. Therefore, a suitable definition of the measurement environment features is a key point for a successful microwave imaging.

Since the targets to be reconstructed have size ranging from few millimeters to some centimeters, data are usually collected at frequencies $f \geq 1\,\mathrm{GHz}$ [2, 7, 8, 11].

At these frequencies, the reflection coefficient at the fluid-skin interface Γ_r has to be taken into account, in order to assure that a suitable fraction of the incident field strikes the internal structures of the breast and then contributes to the overall scattering phenomena.

In this respect, to maximize the incident power, the better choice would be that of using a matching fluid whose conductivity is as low as possible, although a complete absence of losses is not possible to achieve in the case of ultra wide band data. On the other hand, to set the relative permittivity of the matching fluid, let us observe that the investigated scenario can be considered angularly homogeneous and the skin layer is very thin compared to the other involved electrical lengths. Moreover, the breast itself is large in terms of the probing wavelength. As a consequence of these observations, the scattering phenomena can be reasonably described by assuming a three layers one dimensional model [36, 37]. Of course, this simplified model does not take into account the actual complexity of the internal breast structure and the multi scattering effects arising from different breast tissues. However, these effects depend on the specific structure of the female breast and it is not at all straightforward to include them in the framework of an analysis aiming at providing simple and general guidelines. On the other hand, the considered one dimensional model both allows us to deal with a very simple scenario and to take advantage of the transmission line formalism. As a matter of fact, a simple way to evaluate the reflection coefficient Γ_r is to adopt the equivalent transmission line model sketched in Fig. 2. The first part of the transmission line represents the matching fluid (i.e., $Z_f = \sqrt{\mu_0/(\epsilon_0\epsilon_f)}$ is the impedance of the fluid, μ_0 and ϵ_0 being the permeability and the permittivity of vacuum, respectively), the second one corresponds to a damp skin layer 1.5 mm thick and the load impedance schematizes the internal female breast tissues. The complex equivalent permittivities of skin and internal tissues and then their impedances (Z_s and Z_b, respectively) are expressed by using the single pole Cole-Cole model [15, 16].

By doing so, Γ_r is given as:

$$\Gamma_r = \frac{Z_{AA'} - Z_f}{Z_{AA'} + Z_f}, \tag{4}$$

wherein $Z_{AA'}$ is the impedance of the internal breast tissues at the section AA', provided by the impedance transfer equation [27].

It is worth to note that, due to the tissues heterogeneity, the dielectric properties of female breasts are highly variable. However, according to [16], they can be grouped into three main categories, depending on their relative adipose tissue content.

Following this classification, the internal breast structure has been approximated as a homogeneous medium, whose dielectric features depend on its adipose tissue content and are fixed by using the median Cole-Cole parameters provided in [16]. By doing so, three different reflection coefficients have been computed as a function of

the frequency and the relative permittivity of the matching fluid. This latter is supposed to be lossless. Note that such an assumption, which in the following allows us to trace some guidelines to choose the relative permittivity of the matching fluid, will be removed in the numerical examples of Section 5.

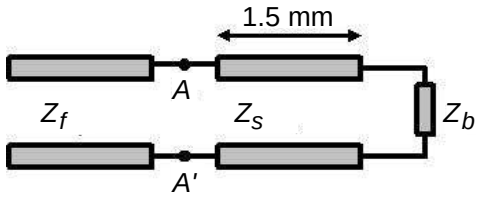

Figure 2. Line transmission model schematizing the breast/matching fluid interface.

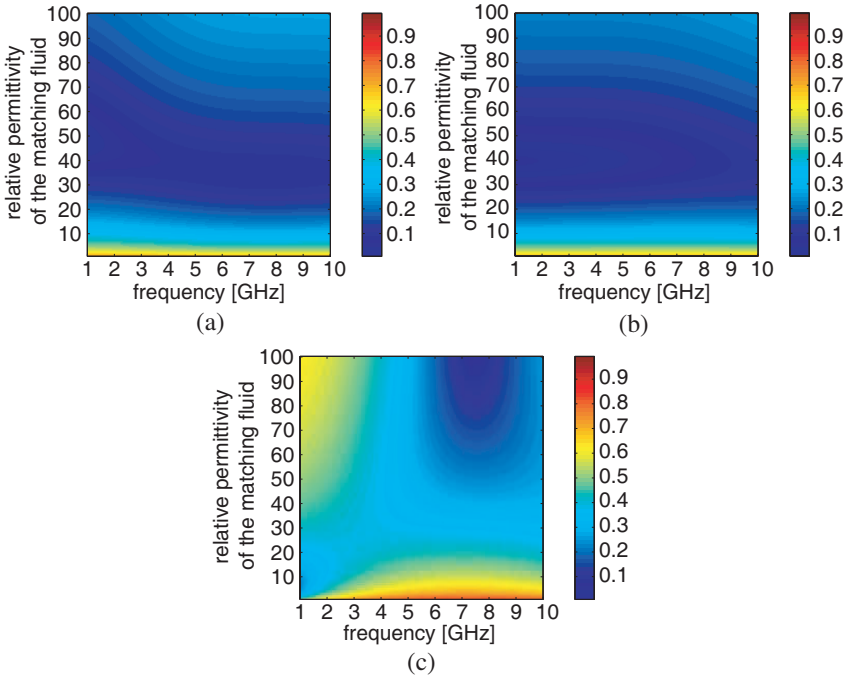

Figure 3. Amplitude of the fluid-skin interface reflection coefficient as a function of the frequency and the relative permittivity of the matching fluid: (a) Breast with 0–30% adipose tissue; (b) Breast with 31–84% adipose tissue; (c) Breast with 85–100% adipose tissue.

The plots of $|\Gamma_r|$ are given in Figs. 3(a)–3(c). These plots show that, as far as breasts having a low (0–30%) or moderate (31–84%) content of adipose tissue are concerned, a relative permittivity $\epsilon_f \geq 10$ is sufficient to ensure a good coupling with the probing waves, such $|\Gamma_r| \leq 0.4$, in the whole frequency range [1–10] GHz. On the contrary, for a breast with high adipose tissue content (85–100%), two unsuitable regions are detected. The first one is for $\epsilon_f > 30$ and low frequencies ($f \in$ [1–4] GHz), while the second one is mainly for $\epsilon_f < 10$ and covers almost all the frequencies range. This result is similar to that in [36].

The plots of $|\Gamma_r|$ given above provide a way to understood how the working frequency and the matching fluid affect the scattering phenomena. On the other hand, they show that there are several possible choices for both ϵ_f and f, so that criteria, related to their expected effects on the imaging process, have to be given.

To this end, one can take into account that the achievable spatial resolution of an imaging method mainly depends on the background wavelength λ_b, being in the order of $\lambda_b/4$ [‡] [38]. On the other hand, the lower is λ_b the larger is the size of the scatterers. As a consequence, the difficulty of the inverse scattering problem becomes higher. As a matter of fact, the *degree of non linearity* of the data to unknown relationship grows with the electrical size of the investigated domain [29, 39, 40]. Therefore, one should choose the working frequencies as well as ϵ_f as a trade-off between these two opposite requests.

In this respect, the plots of $|\Gamma_r|$ suggest that, whatever is the adipose tissue content of the probed breast, a suitable choice should be a matching fluid with $\epsilon_f \in$ [10–30]. Moreover, by taking into account that the complexity of the inverse problem as well as the increase of the spatial resolution with ϵ_f, it seems convenient set ϵ_f approximately equal to the medium value of the indicated range. As it is stressed by the following numerical analysis, this seems a general guideline for assuring a reliable characterization of the internal breast tissues.

The plots of the reflection coefficients suggest that, provided the matching fluid is properly chosen, a good coupling between the wave and the target is achievable already at the lower frequencies. Therefore, one can meet the trade-off between the robustness of the inversion approach against local minima and the achievable spatial resolution by collecting the data in the low part of the spectrum considered in the plots starting from 1 GHz. It is worth to remark that the electric size of the investigated domain and then the complexity of the inverse scattering problem at hand grow with the frequency [39]. In particular,

[‡] This value is the exact one for the Born Approximation [38], whereas it can be considered as an upper bound for the general (non-linear) case, if one takes into account that the number of degrees of freedom of data enforces a limit on the maximum number of parameters (describing the inclusions) which can be safely extracted [32].

our numerical experience suggests that, as far as the adopted inversion procedure is concerned, data collected from 1 GHz to 3.5 GHz are suitable to image all the three typologies of breast. Of course, the use of a different inversion strategy may allow to consider a different frequency range. On the other hand, for a given measurement device, a more accurate choice of the working frequencies to process can be done by taking into account the specific properties of the matching material actually realized and the performance of the adopted antennas.

The last issue to address is the choice of the number N of transmitting and receiving probes. This latter should be chosen in order to collect as much independent information as possible, while avoiding redundant measures. To this end, one can take advantage of the spatial band-limitedness of the scattered fields [32–34], which allows to fix the optimal number and the position of the sampling points needed to accurately represent the field. In particular, when considering a circumference as measurement domain (like in the case at hand) and assuming that Ω is enclosed in a circle of radius a, these results suggest that the sampling points have to be angularly equispaced with spacing $\Delta\theta = \lambda/2a$. As far as the transmitters are concerned, the aim is to consider all possible independent scattering experiments in order to improve the robustness of the imaging process against false solutions occurrence [32], while not increasing the complexity of the inverse problem and the measurement device. By taking advantage of Lorentz reciprocity, one can apply the same criterion as above to give an upper bound to the number of scattering experiments to be considered, i.e., for the number of the transmitting probes.

Accordingly, one can set the number of probes $N \geq 2\beta_b\, a + 1$, β_b being the real part of the wave number at the considered frequency [32]. Since N depends on the frequency, to collect multifrequency data one should (in principle) modify the number of probes at each considered frequency. Of course, this is unpractical. In addition, to reduce the coupling effects among the probes, N should be kept as low as possible. Taking into account these considerations and the advantages offered by the use of the frequency hopping strategy, we set $N \geq N_{\min}$, $N_{\min}$ being the number of probes corresponding to the lowest wave number. This is corroborated by the following numerical analysis.

5. NUMERICAL EXAMPLES

In order to assess the effectiveness of the proposed guidelines against realistic scenarios, the numerical breast phantom repository given in [24] has been exploited. Such a database provides anatomically

realistic 3D numerical phantoms from NMR images, so 2D breast models have been obtained by considering only a slice of the selected phantoms.

According to the statements given in the previous section and considering the radius of the circle surrounding the investigated domain equal to 14 cm, $N = 30$ equispaced transmitting and receiving probes located all around Ω on a circle having radius of 19 cm have been considered. The synthetic data have been generated in the frequency range 1–3.5 GHz with $\Delta_f = 250$ MHz by means of a method of moments based full wave forward solver and corrupted by an additive Gaussian noise with SNR = 30 dB. Note that, unlike what we assumed in the inversion scheme (see Section 3), the data have been generated by using the single pole Cole-Cole model to accurately describe the dispersive behavior of the breast tissues. In particular, the frequency-dependent dielectric properties of each pixel of the considered breast phantoms have been assigned following the instructions provided in [24].

To quantify the accuracy of the obtained reconstructions, we have considered the normalized reconstruction error:

$$err = \frac{\|\tilde{\chi} - \chi\|^2}{\|\chi\|^2}, \tag{5}$$

$\tilde{\chi}$ being the reconstructed contrast function and χ the reference one.

The starting point of the iterative inversion procedure at 1 GHz is obtained by assigning at the breast' shape given by the LSM a relative permittivity equal to 10 and a conductivity of 20 mS/m.

The first example concerns a breast having a moderate adipose content. In this respect, the slice $s_1 = 150$ of the fibroglandular breast (breast ID: 070604PA1) [24] has been considered, s_1 denoting the horizontal slices of the 3D phantom.

In order to show the importance of a proper choice of the matching fluid, we have processed data collected without matching fluid ($\epsilon_f = 1$, $\sigma_f = 0$ S/m) and by using liquids having $\epsilon_{f2} = 18$ and $\epsilon_{f3} = 35$, respectively. Moreover, since it is unrealistic to have a completely lossless liquid, we have adopted a maxwellian model to describe its dispersive features and set $\sigma_f = 10$ mS/m, in these last cases.

The reconstruction errors at 1 GHz, that is the first processed frequency, are given in Table 1. These results clearly state that the inversion strategy provides an inaccurate reconstruction when no matching fluid is used, since there is not a good coupling among the incident waves and the internal breast tissues, being $|\Gamma_r| > 0.5$. Moreover, a completely unreliable result is attained by using a liquid with $\epsilon_f = 35$ and $\sigma_f = 10$ mS/m, due to the increased non linearity of the inverse scattering problem [40]. Similar results are

foreseeable for liquids having $\epsilon_f > 35$. On the other hand, a functional characterization of the breast tissues is actually possible by using a liquid with relative permittivity in the selected range ($\epsilon_f = 18$), as it is corroborated by Figs. 4(a)–4(d), where the reference permittivity and conductivity profiles as well as the reconstructed ones at the higher processed frequency are shown. In this case, the dielectric properties of the adipose tissue are well reconstructed and the fibroglandular one is detected, well located and its properties are retrieved with good approximation. It is must be observed that, the skin layer is

Table 1. Fibroglandular breast — Reconstruction errors for different permittivities of the matching fluid at 1 GHz.

	$err_{\epsilon_f=1}$	$err_{\epsilon_f=18}$	$err_{\epsilon_f=35}$
1 GHz	0.90	0.43	1.25

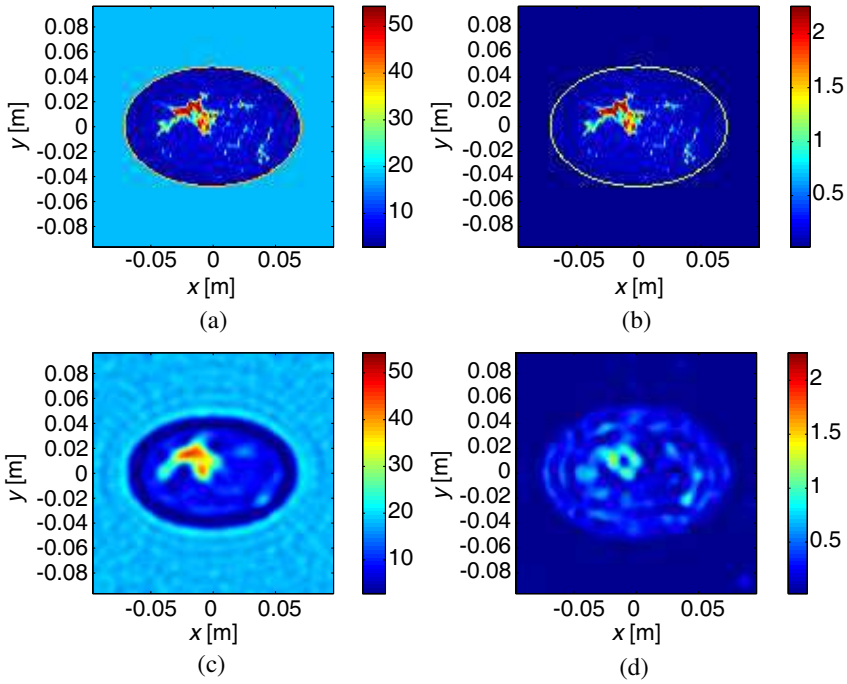

Figure 4. Fibroglandular breast: (a) Reference relative permittivity; (b) Reference conductivity [S/m]; (c) Reconstructed relative permittivity; (d) Reconstructed conductivity [S/m].

missed because its electrical thickness is too small and lower than the attainable resolution limit of the inversion procedure. The normalized reconstruction errors at some frequencies are given in Table 2.

As a second example, a breast having a low adipose content has been taken into account. In particular, the numerical phantom corresponds to the slice $s_1 = 150$ of the heterogeneous dense breast (Breast ID = 070604PA2) [24]. Fig. 5 shows the reference permittivity and conductivity profiles as well as the reconstructed ones at the higher processed frequency, for a matching fluid having $\epsilon_f = 18$ and

Table 2. Fibroglandular breast — Reconstruction errors at different frequencies ($\epsilon_f = 18$ and $\sigma_f = 10\,\mathrm{mS/m}$).

	1 GHz	1.5 GHz	2 GHz	2.5 GHz	3 GHz	3.5 GHz
$err_{\epsilon_f=18}$	0.43	0.35	0.33	0.31	0.30	0.30

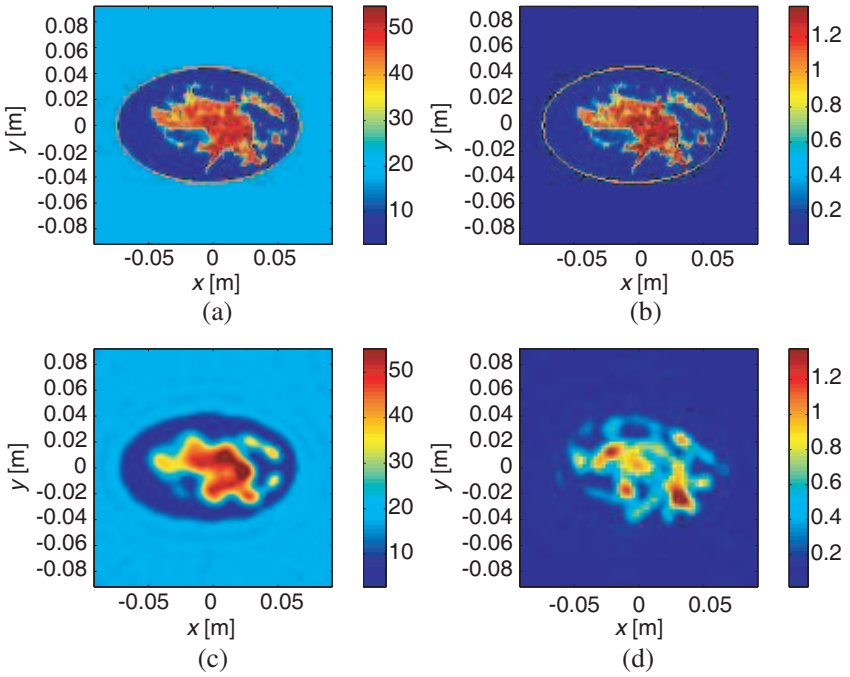

Figure 5. Heterogeneous dense breast: (a) Reference relative permittivity; (b) Reference conductivity [S/m]; (c) Reconstructed relative permittivity; (d) Reconstructed conductivity [S/m].

$\sigma_f = 10\,\mathrm{mS/m}$. The reconstruction errors are given in Table 3. As in the previous example, a satisfactory morphological and functional reconstruction of the internal breast tissues is achieved.

The last example concerns a mostly fatty female breast (Breast ID: 0.1904, $s_1 = 150$) [24]. Also in this case, the internal breast tissues are well retrieve by setting $\epsilon_f = 18$ and $\sigma_f = 10\,\mathrm{mS/m}$, see Figs. 6(a)–6(d). As a matter of fact, from Figs. 6(c) and 6(d) one can conclude that the breast exhibits a high adipose tissue content and detect and locate the fibroglandular tissues. The reconstruction errors at different processed frequencies are given in Table 4.

Table 3. Heterogeneous dense breast — Reconstruction errors at different frequencies ($\epsilon_f = 18$ and $\sigma_f = 10\,\mathrm{mS/m}$).

	1 GHz	1.5 GHz	2 GHz	2.5 GHz	3 GHz	3.5 GHz
$err_{\epsilon_f=18}$	0.42	0.35	0.32	0.31	0.31	0.31

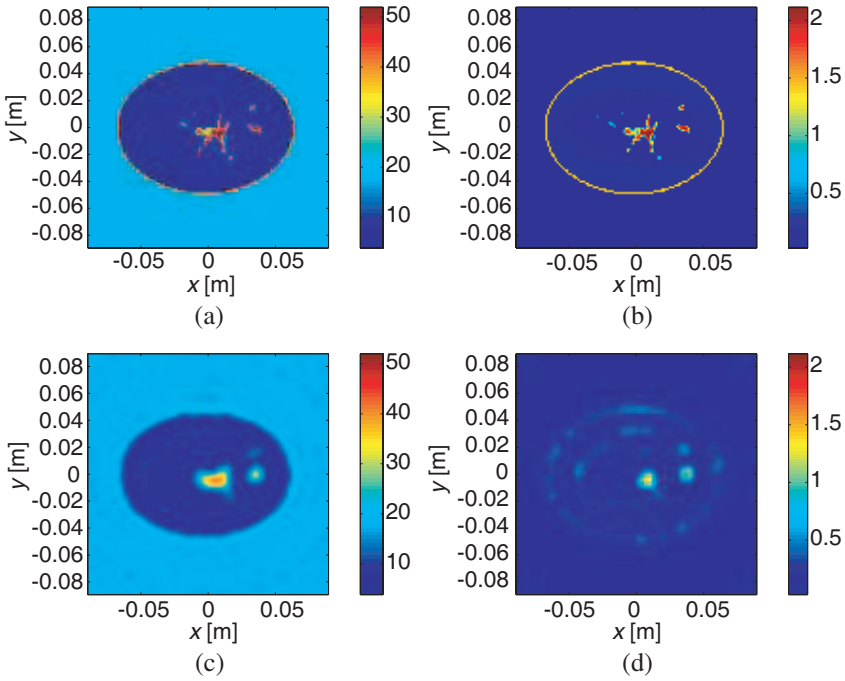

Figure 6. Mostly fatty breast: (a) Reference relative permittivity; (b) Reference conductivity [S/m]; (c) Retrieved relative permittivity; (d) Retrieved conductivity [S/m].

Table 4. Mostly fatty breast — Reconstruction errors at different frequencies ($\epsilon_f = 18$ and $\sigma_f = 10\,\mathrm{mS/m}$).

	1 GHz	1.5 GHz	2 GHz	2.5 GHz	3 GHz	3.5 GHz
$err_{\epsilon_f=18}$	0.42	0.36	0.34	0.31	0.29	0.29

6. CONCLUSION

In this paper the factors affecting accuracy and effectiveness of microwave techniques for breast imaging have been investigated and some guidelines have been traced to address the design of improved screening tools. In particular, by exploiting a simplified model, we have achieved some useful guidelines to set matching fluid, frequency range and number of transmitting and receiving probes such to assure satisfactory reconstruction capabilities. The effectiveness of these guidelines has been assessed by means of a numerical analysis dealing with synthetic data and referred to two-dimensional anthropomorphic numerical breast phantoms. In particular, the dielectric properties of breast tissues have been reconstructed from multiview, multistatic and multifrequency data by means of a two step approach. This last jointly uses the LSM and an iterative inversion procedure, that is based on the CSI strategy and exploits the regularization by projection and the frequency hopping procedure.

The achieved results assess the feasibility of a morphological and functional characterization of the internal breast tissues. In the framework of breast cancer screening, such a characterization provides a crucial a priori information which can be exploited to improve the imaging capabilities of diagnostics approaches.

Future activities will be devoted to tackle the more realistic 3D case and to address the design of a microwave imaging tool for early stage breast cancer detection. Also, we will integrate the proposed guidelines by taking into account a more complex model of the scattering scenario, including the dispersive behaviour of biocompatible matching fluids and the radiation patterns of the antennas.

ACKNOWLEDGMENT

This work has been partially supported by the Italian Ministry of Research under the Program PRIN 2007, "MANFIND: Magnetic Nanoparticles and Fields for Nanotechnologies and Diagnostics". The authors wish to thank Dr. Michele D'Urso for useful discussions.

REFERENCES

1. Fear, E. C., P. M. Meaney, and M. A. Stuchly, "Microwaves for breast cancer detection," *IEEE Potentials*, 2003.
2. Zhang, H., S. Y. Tan, and H. S. Tan, "A novel method for microwave breast cancer detection," *Progress In Electromagnetics Research*, PIER 83, 413–434, 2008.
3. Bindu, G., S. J. Abraham, A. Lonappan, V. Thomas, C. K. Aanandan, and K. T. Mathew, "Active microwave imaging for breast cancer detection," *Progress In Electromagnetics Research*, PIER 58, 149–169, 2006.
4. Lazaro, A., D. Girbau, and R. Villarino, "Simulated and experimental investigation of microwave imaging using UWB," *Progress In Electromagnetics Research*, PIER 94, 263–280, 2009.
5. Huynh, P. T., A. M. Jarolimek, and S. Dayee, "The false-negative mammogram," *Radiographics*, Vol. 18, 1137–1154, 1998.
6. Christiansen, C. L., F. Wang, M. B. Barton, W. Kreuter, J. G. Elmore, A. E. Gelfand, and S. W. Fletcher, "Predicting the cumulative risk of false-positive mammograms," *Nat. Cancer Inst. J.*, Vol. 92, 1373–1380, 2000.
7. Li, X., S. K. Davis, S. C. Hagness, D. W. Van Der Weide, and B. D. Van Veen, "Microwave imaging via space-time beamforming: Experimental investigation of tumor detection in multilayer breast phantoms," *IEEE Trans. Microw. Theory Tech.*, Vol. 52, 1856–1865, 2004.
8. Williams, T. C., E. C. Fear, and D. T. Westwick, "Tissue sensing adaptive radar for breast cancer detection-investigations of an improved skin-sensing method," *IEEE Trans. Microw. Theory Tech.*, Vol. 54, 1308–1313, 2006.
9. Zainud-Deen, S. H., W. M. Hassen, E. El deen Ali, and K. H. Awadalla, "Breast cancer detection using a hybrid finite difference frequency domain and particle swarm optimization techniques," *Progress In Electromagnetics Research B*, Vol. 3, 35–46, 2008.
10. Meaney, P. M., M. W. Fanning, T. Raynolds, et al., "Initial clinical experience with microwave breast imaging in women with normal mammography," *Academic Radiology*, Vol. 14, 207–218, 2007.
11. Rubk, T., P. M. Meaney, P. Meincke, and K. D. Paulsen, "Nonlinear microwave imaging for breast-cancer screening using GaussNewton's method and the CGLS inversion algorithm," *IEEE Trans. Antennas Propag.*, Vol. 55, 2320–2231, 2007.
12. De Zaeytijd, J., C. L. Conmeaux, and A. Franchois, "Three-

dimensional linear sampling applied to microwave breast imaging," *29th General Assembly of the International Union of Radio Science (URSI)*, Chicago, USA, August 7–16, 2008.

13. Zhou, H., T. Takenaka, J. E. Johnson, and T. Tanaka, "A breast imaging model using microwaves and a time a domain three dimensional reconstruction," *Progress In Electromagnetics Research*, PIER 93, 57–70, 2009.
14. Gilmore, C., A. Abubakar, W. Hu, T. M. Habashy, and P. M. Van Den Berg, "Microwave biomedical data inversion using the finite-difference contrast source inversion method," *IEEE Trans. Antennas Propag.*, Vol. 57, 1528–1538, 2009.
15. Gabriel, S., R. W. Lau, and C. Gabriel, "The dielectric properties of biological tissues: 3. Parametric models for the dielectric spectrum of tissues," *Phys. Med. Biol.*, Vol. 41, 2271–2293, 1996.
16. Lazebnik, M., L. McCartney, D. Popovic, C. B. Watkins, M. J. Lindstrom, J. Harter, S. Sewall, A. Magliocco, J. H. Booske, M. Okoniewski, and S. C. Hagness, "A large-scale study of the ultrawideband microwave dielectric properties of normal breast tissue obtained from reduction surgeries," *Phys. Med. Biol.*, Vol. 52, 2637–2656, 2007.
17. Lazebnik, M., D. Popovic, L. McCartney, C. B. Watkins, M. J. Lindstrom, J. Harter, S. Sewall, T. Ogilvie, A. Magliocco, T. M. Breslin, W. Temple, D. Mew, J. H. Booske, M. Okoniewski, and S. C. Hagness, "A large-scale study of the ultrawideband microwave dielectric properties of normal, benign and malignant breast tissue obtained from cancer surgeries," *Phys. Med. Biol.*, Vol. 52, 6093–6115, 2007.
18. Mashal, A., B. Sitharaman, J. H. Booske, S. C. Haghness, "Dielectric characterization of carbons nanotube contrast agents for microwave breast cancer detection," *2009 IEEE Int. Symp. on Antennas and Propag. & USNC/URSI National Radio Sci. Meeting*, Charleston, SC, USA, June 1–5, 2009.
19. Zhao, M., S. C. Haghness, B. D. Van Veen, and D. W. Van Der Weide, "Computational study of a focused acustic and microwave hybrid sensing modality that exploits coupled and elastic properties contrasts," *2009 IEEE Int. Symp. on Antennas and Propag. & USNC/URSI National Radio Sci. Meeting*, Charleston, SC, USA, June 1–5, 2009.
20. Abbosh, A., "Early breast cancer detection using hybrid imaging modality," *2009 IEEE Int. Symp. on Antennas and Propag. & USNC/URSI National Radio Sci. Meeting*, Charleston, SC, USA, June 1–5, 2009.

21. Bertero, M. and P. Boccacci, *Introduction to Inverse Problems in Imaging*, Inst. of Physics, Bristol Philadelphia, UK, 1998.
22. Li, F., X. Chen, and K. Huang, "Microwave imaging a buried object by the GA and using the S_{11} parameter," *Progress In Electromagnetics Research*, PIER 85, 289–302, 2008.
23. Meng, Z. Q., "Autonomous genetic algorithm for functional optimization," *Progress In Electromagnetics Research*, PIER 72, 253–268, 2007.
24. Zastrow, E., S. K. Davis, M. Lazebnik, F. Kelcz, B. D. Van Veem, and S. C. Hagness, "Database of 3D grid-based numerical breast phantom for use in computational electromagnetics simulations," http://uwcem.ece.wisc.edu\home.htm.
25. Colton, D., H. Haddar, and M. Piana, "The linear sampling method in inverse electromagnetic scattering theory," *Inv. Ploblems*, Vol. 19, S105–S137, 2003.
26. Isernia, T., V. Pascazio, and R. Pierri, "On the local minima in a tomographic imaging technique," *IEEE Trans. Geosci. Rem. Sens.*, Vol. 39, 1596–1607, 2001.
27. Balanis, C. A., *Advanced Enginnering Electromagnetics*, John Wileys & Sons, 1989.
28. Catapano, I., L. Crocco, and T. Isernia, "On simple method for shape reconstruction of unknown scatters," *IEEE Trans. Antennas Propag.*, Vol. 55, 1431–1436, 2007.
29. Catapano, I., L. Crocco, M. D'Urso, and T. Isernia, "On the effect of support estimation and of a new model in 2-D inverse scattering problems," *IEEE Trans. Antennas and Propag.*, Vol. 55, 1895–1899, 2007.
30. Van Den Berg, M. and A. Abubakar, "Contrast source inversion method: State of art," *Progress In Electromagnetics Research*, PIER 34, 189–218, 2001.
31. Tikhonov, A. N., A. V. Goncharky, V. V. Stepanov, and A. G. Yagola, *Numerical Methods for the Solution of Ill-posed Problems*, Dordrecht, Kluver, 1995.
32. Bucci, O. M. and T. Isernia, "Electromagnetic inverse scattering: Retrievable information and measurement strategies," *Radio Sci.*, Vol. 32, 2123–2137, 1997.
33. Bucci, O. M. and G. Franceschetti, "On the degree of feedom of scattered fields," *IEEE Trans. Antennas Propag.*, Vol. 37, 918–926, 1989.
34. Bucci, O. M., L. Crocco, and T. Isernia, "Improving the reconstruction capabilties in inverse scattering problems by

exploitation of close-proximity setup," *J. Opt. Soc. Am. A*, Vol. 16, 1788–1798, 1999.

35. Chew, W. C. and J. C. Lin, "A frequency-hopping approach for microwave imaging of large inhomogeneous bodies," *IEEE Microw. Guided Wave Lett.*, Vol. 5, 439–441, 1995.
36. Rappaport, C., "Determination of bolus dielectric constrant for optimum coupling of microwaves through skin for breast cancer imaging," *Int. J. of Antennas and Propag.*, Vol. 2008, 2008.
37. Catapano, I., L. Crocco, M. DUrso, A. Morabito, and T. Isernia, "Microwave tomography of breast cancer: A feasibility study," *European Conf. on Antennas and Propag. (EuCAP)*, Nice, France, November 6–10, 2006.
38. Slaney, M., A. C. Kak, and L. E. Larsen, "Limitations of imaging with first-order diffraction tomography," *IEEE Trans. on Microw. Theory Tech.*, Vol. 32, 860–874, 1984.
39. Bucci, O. M., N. Cardace, L. Crocco, and T. Isernia, "Degree of non-linearity and a new solution procedure in scalar 2-D inverse scattering problems," *J. Opt. Soc. Am. A*, Vol. 18, 1832–1845, 2001.
40. Isernia, T., L. Crocco, and M. D'Urso, "New tools and series for forward and inverse scattering problems in lossy media," *IEEE Geosci. Remote Sens. Letters*, Vol. 1, 327–331, 2004.